

Developments in Heterobimetallic s-Block Systems: Synthesis and Structural Survey of Molecular M/Ae (M = Li, Na, K, Cs; Ae = Ca, Sr) Aryloxo Complexes

Maria Felisa Zuniga,[†] Glen B. Deacon,[‡] and Karin Ruhlandt-Senge^{*†}

Department of Chemistry, 1-014 Center for Science and Technology, Syracuse University, Syracuse, New York 13244-4100, and School of Chemistry, Monash University, Victoria 3800, Australia

Received December 20, 2007

A series of novel heterobimetallic group 1/strontium and group 1/calcium aryloxo complexes having the composition [MAe(Odpp)₃] [Ae = Sr and M = Na (1), K (2, 3), Cs (4); Ae = Ca and M = Na (5), K (6), Cs (7)] or [M₂Ae(Odpp)₄] [M = Li and Ae = Sr (9), Ca (10)] have been prepared using 2,6-diphenylphenol (HOdpp) as the ligand. Through the use of solid-state direct metalation, these compounds were obtained either directly from the reaction vessel or after workup in toluene. The Lewis base adduct [KCa(Odpp)₃(thf)] (8) was obtained by treatment of [KCa(Odpp)₃] (6) with tetrahydrofuran (thf). All of the compounds displayed extensive metal– π -arene interactions, which provide significant stabilization in these reactive species. The thermal stabilities and volatilities of representative heterobimetallic strontium and calcium complexes were investigated using thermogravimetric analysis.

Introduction

The interest in heterobimetallic complexes involving s-block elements has been motivated by their distinctive and enhanced reactivity compared with that of their homometallic analogues. This important phenomenon is best exemplified by mixtures of organolithium compounds and sodium or potassium alkoxides, which merited the term “superbases” on the basis of their superior deprotonating ability compared with that of the parent lithium compounds.^{1,2} Similarly, recent seminal works on heterobimetallic alkali/magnesium compounds, including investigations of their solid-state structures and unique chemical properties compared with those of magnesium-only compounds, have opened exciting opportunities in synthetic chemistry.^{3,4} Our contribution in this area consisted of the structural characterization of a series of lithium aryloxo magnesiates that exhibit various Li/Mg

ratios and ion-association modes, which are influenced by the size of the ligand as well as the type of donor solvents.⁵

In contrast to the voluminous literature on heterobimetallic magnesium species, reports on well-characterized mixed s-block complexes involving the heavy alkaline earth metals are limited.^{6,7} As in the case of mixed-metal alkali systems, efforts to synthesize heterobimetallic compounds of alkaline earth metals are challenged by their tendency to form mixtures of homometallic species, as verified in our work as well as by others. A small number of alkali/calcium complexes have been previously reported, typically displaying the 1:1 formulation also commonly observed for the magnesium species. Examples include [LiCa{ μ -N(SiMe₃)₂]₂[N(SiMe₃)₂]}⁸ and its solvated analogue [Li(thf)Ca{ μ -N(SiMe₃)₂]₂[N(SiMe₃)₂]} (thf = tetrahydrofuran),⁹ the polymeric species [K(thf)Ca{ μ -N(SiMe₃)₂]₂[N(SiMe₃)₂]}_∞,¹⁰ and the enolates [K₂Ca₂{OC(Mes)=CH₂}]₆¹⁰ and [K₂Ca{OC(Mes)=CH₂}]₄.¹⁰ More recently, Fromm and

* To whom correspondence should be addressed. E-mail: kruhland@syr.edu. Phone: 315-443-1306. Fax: 315-443-4070.

[†] Syracuse University.

[‡] Monash University.

(1) Lochmann, L. *Eur. J. Inorg. Chem.* **2000**, 1115–1126.

(2) Schlosser, M. *Pure Appl. Chem.* **1988**, *60*, 1627–1634.

(3) Mulvey, R. E. *Organometallics* **2006**, *25*, 1060–1075.

(4) Mulvey, R. E.; Mongin, F.; Uchiyama, M.; Kondo, Y. *Angew. Chem., Int. Ed.* **2007**, *46*, 3802–3824.

(5) Zuniga, M. F.; Kreutzer, J.; Teng, W.; Ruhlandt-Senge, K. *Inorg. Chem.* **2007**, *46*, 10400–10409.

(6) Westerhausen, M. *Dalton Trans.* **2006**, 4755–4768.

(7) Fromm, K. M.; Gueneau, E. D. *Polyhedron* **2004**, *23*, 1479–1504.

(8) Kennedy, A. R.; Mulvey, R. E.; Rowlings, R. B. *J. Organomet. Chem.* **2002**, *648*, 288–292.

(9) Davies, R. P. *Inorg. Chem. Commun.* **2000**, *3*, 13–15.

(10) He, X.; Noll, B. C.; Beatty, A.; Mulvey, R. E.; Henderson, K. W. *J. Am. Chem. Soc.* **2004**, *126*, 7444–7445.

co-workers reported a series of solvated mixed alkali/alkaline earth metal alkoxy and aryloxy compounds depicted as multinuclear arrangements, namely, $[\{\text{Li}(\text{thf})\}_4\text{Ae}(\text{OtBu})_4(\text{OH})\text{-}(\text{I})]$ (Ae = Ca, Sr, Ba),^{11–14} $[\text{M}_6\text{Ae}(\text{C}_6\text{H}_5\text{O})_8(\text{thf})_6]$ (M = Li, Na; Ae = Ca, Sr, Ba),^{13,15} $[\text{M}_2\text{Ca}_2(\text{C}_6\text{H}_5\text{O})_6(\text{dme})_4]$ (M = Li, Na; dme = dimethoxyethane),^{13,15} $[\text{Li}(\text{thf})_4][\{\text{Sr}_6(\text{OtBu})_7(\mu_3\text{-D})(\text{I})_2(\text{thf})_3\}_2(\mu\text{-I})]$,¹⁶ $[\text{Li}_6\text{Ca}(\text{OPh})_6(\text{OtBu})_2(\text{thf})_6]$,¹³ and $[(\mu\text{-dme})\{\text{Li}_6\text{Sr}(\text{OPh})_8(\text{thf})_{4-n}(\text{dme})_n\}]$ ($n = 0, 2$).¹³ With the heavier strontium and barium congeners, other cluster-type molecular heterobimetallic compounds containing oxide (O^{2-}) include $[(\text{Li}_3\text{Ba}_6\text{O}_2)(\text{OtBu})_{11}(\text{thf})_3]$ ¹⁷ and $[\text{Na}_2\text{Ba}\{\text{p-}t\text{Bu-calix[4]}(\text{OC}_5\text{H}_9)_2(\text{O})_2\}_2]$.¹⁸ We recently described a family of M/Ba (M = Li, Na, K, Cs) complexes of simple formulation, namely, $[\text{MBa}(\text{Odpp})_3]$ and $[\text{M}_2\text{Ba}(\text{Odpp})_4]$.¹⁹

We are now extending our work on heterobimetallic alkali/alkaline earth metal aryloxides toward the calcium and strontium derivatives. Our aim is to systematically investigate structural trends within this group of compounds by using 2,6-diphenylphenol (HODpp) as the ligand, as we did previously for the related barium compounds. In view of the finding that the barium congeners displayed extensive metal– π interactions, we intend to obtain further insights into the role of secondary interactions in the stabilization of the lighter alkaline earth metal analogues. Since homometallic alkaline earth metal alkoxy and aryloxy compounds have been the topic of investigations related to the preparation of advanced materials, in this work we performed preliminary screenings of the heterobimetallic compounds as precursors for metal oxides by metal–organic chemical vapor deposition (MOCVD) techniques.^{20–22} The target compounds were subjected to thermogravimetric analysis, allowing the correlation of thermal stability and alkali/alkaline earth metal composition.

Use of the alkali metals sodium, potassium, and cesium (M) in combination with the alkaline earth metals strontium and calcium (Ae) gave compounds having the general composition $[\text{MAe}(\text{Odpp})_3]$, while introduction of lithium afforded species with a 2:1 metal ratio having the formula $[\text{M}_2\text{Ae}(\text{Odpp})_4]$. Herein we present a series of donor-free M/Sr and M/Ca compounds as well as one THF-solvated species, as summarized in Table 1. These compounds were

Table 1. List of Compounds

M/Sr		M/Ca	
	[MAe(Odpp) ₃]		
[NaSr(Odpp) ₃]·PhMe	1	[NaCa(Odpp) ₃]·PhMe	5
[KSr(Odpp) ₃]	2	[KCa(Odpp) ₃]	6
[KSr(Odpp) ₃]·PhMe	3	[CsCa(Odpp) ₃]	7
[CsSr(Odpp) ₃]	4	[KCa(Odpp) ₃ (thf)]·PhMe	8
	[M ₂ Ae(Odpp) ₄]		
[Li ₂ Sr(Odpp) ₄]·PhMe	9	[Li ₂ Ca(Odpp) ₄]·hexane	10

prepared by solid-state direct metalation, a synthetic route developed for the preparation of rare earth complexes.²³

Experimental Section

All manipulations were carried out under an inert gas atmosphere using standard Schlenk line techniques or a Braun Labmaster 100 drybox because of the extremely air- and moisture-sensitive nature of the compounds described herein. 2,6-Diphenylphenol was purchased and used as received. MODpp (M = Li, Na, K, Cs)²⁴ and 1,3,5-tri-*tert*-butylbenzene (Mes*H)²⁵ were prepared according to literature procedures. All of the solvents were purified using standard procedures. ¹H NMR spectra were recorded using a Bruker DPX 300 spectrometer. IR spectra (4000–650 cm⁻¹) were recorded as Nujol mulls between KBr plates using a Nicolet IR200 spectrometer. Metal analyses were determined by Complete Analysis Laboratories, Inc. (Parsippany, NJ). Thermal analysis was performed using a TA Instruments high-resolution TGA 2950 thermogravimetric analyzer; TGA data were collected using Thermal Advantage software, version 1.1A. Carius tubes were charged with the starting materials, sealed under vacuum (50 mtorr), and heated in a furnace. The tubes were cooled to room temperature and placed in the glovebox, where the crude product was transferred to a Schlenk flask and washed with hexane (2 × 30 mL) to remove Mes*H.

Caution! During the solid-state reactions employed in this work, H₂ gas is generated. Accordingly, reaction scales must be adjusted in order to avoid exceeding a pressure of 15 atm when using heavy-walled Carius glass tubes. Furthermore, safety precautions (such as using a metal sleeve) must be applied when transporting the Carius tubes into the glovebox.

Crystals suitable for single-crystal X-ray diffraction were obtained (a) by recrystallization from toluene (for **1**, **3**, **5**, **9**, and **10**), (b) from the crystalline materials deposited on top of the tube (for **2**, **4**, **6**, and **7**), or (c) as described below for **8**. Crystallographic analyses for all of the compounds were conducted as described previously.²⁶ Disorder was handled by introducing split positions: 50:50 for K and Sr metal centers in **3**; 80:20 for one of the aryloxy ligands in **6**; and 60:40 for the THF donor in **8**. Some severely disordered solvents of crystallization (particularly PhMe in **1**, **3**, **5**, **8**, and **9** and hexane in **10**) were removed from the refinement using the PLATON software package.^{27,28} Crystallographic data (excluding structure factors) for the structures reported herein have been deposited in the Cambridge Crystallographic Data Center (CCDC deposition numbers 669644–669653). CIF files can be obtained

- Fromm, K. M.; Gueneau, E. D.; Bernardinelli, G.; Goesmann, H.; Weber, J.; Mayor-Lopez, M. J.; Boulet, P.; Chermette, H. *J. Am. Chem. Soc.* **2003**, *125*, 3593–3604.
- Fromm, K. M.; Gueneau, E. D.; Goesmann, H. *Chem. Commun.* **2000**, 2187–2188.
- Maudez, W.; Meuwly, M.; Fromm, K. M. *Chem.—Eur. J.* **2007**, *13*, 8302–8316.
- Fromm, K. M.; Gueneau, E. D.; Robin, A. Y.; Maudez, W.; Sague, J.; Bergougnant, R. *Z. Anorg. Allg. Chem.* **2005**, *631*, 1725–1740.
- Maudez, W.; Haussinger, D.; Fromm, K. M. *Z. Anorg. Allg. Chem.* **2006**, *632*, 2295–2298.
- Maudez, W.; Vig-Slentes, T.; Mirolo, L.; Fleury, A.; Fromm, K. M. *Main Group Chem.* **2006**, *5*, 41–49.
- Bock, H.; Hauck, T.; Naether, C.; Roesch, N.; Stauffer, M.; Haeblerl, O. D. *Angew. Chem., Int. Ed. Engl.* **1995**, *34*, 1353–1355.
- Guillemot, G.; Solari, E.; Rizzoli, C.; Floriani, C. *Chem.—Eur. J.* **2002**, *8*, 2072–2080.
- Zuniga, M. F.; Deacon, G. B.; Ruhlandt-Senge, K. *Chem.—Eur. J.* **2007**, *13*, 1921–1928.
- Bradley, D. C. *Chem. Rev.* **1989**, *89*, 1317–1322.
- Caulton, K. G.; Hubert-Pfalzgraf, L. G. *Chem. Rev.* **1990**, *90*, 969–995.
- Hubert-Pfalzgraf, L. G. *Inorg. Chem. Commun.* **2003**, *6*, 102–120.

- Deacon, G. B.; Forsyth, C. M. In *Inorganic Chemistry Highlights*; Meyer, G., Naumann, D., Wesemann, L., Eds.; Wiley-VCH: Weinheim, Germany, 2002; Chapter 7.
- Weinert, C. S.; Fanwick, P. E.; Rothwell, I. P. *Inorg. Chem.* **2003**, *42*, 6089–6094.
- Baas, J. M. A.; Van Bekkum, H.; Hoefnagel, M. A.; Wepster, B. M. *Recl. Trav. Chim. Pays-Bas* **1969**, *88*, 1110–1114.
- Ruhlandt-Senge, K.; Englisch, U. *Chem.—Eur. J.* **2000**, *6*, 4063–4070.

from the CCDC free of charge via http://www.ccdc.cam.ac.uk/data_request/cif.

[NaSr(Odpp)₃]·PhMe (1). Sr (0.44 g, 5.0 mmol), HOdpp (0.50 g, 2.0 mmol), NaOdpp (0.27 g, 1.0 mmol), and Mes*H (0.5 g, 2.0 mmol) were heated to 225 °C for 6 days. The crude product was dissolved in hot toluene (PhMe) (20 mL), and the solution was filtered while hot to remove excess metal. Cooling the yellow solution to room temperature overnight afforded colorless crystals. Yield: 0.53 g (59%). Mp (sealed tube/N₂): 248–254 °C. ¹H NMR (300 MHz, benzene-*d*₆, 25 °C): δ 2.11 (s, 3H, CH₃–PhMe), 6.73 [t, 6H, *p*-H(Ph)], 6.79 (t, 3H, *p*-aryl-H), 6.87 [t, 12H, *m*-H(Ph)], 7.15 (m, 2.5H, aryl-PhMe), 7.32 (d, 6H, *m*-aryl-H), 7.45 [d, 12H, *o*-H(Ph)]. IR (Nujol) ν (cm⁻¹): 2920 (s), 2853 (s), 1953 (w), 1896 (w), 1592 (m), 1582 (m), 1554 (m), 1495 (m), 1453 (s), 1413 (s), 1378 (m), 1297 (s), 1255 (m), 1173 (w), 1155 (w), 1108 (w), 1070 (m), 1025 (w), 1010 (m), 991 (w), 919 (w), 853 (s), 800 (w), 766 (s), 754 (s), 731 (m), 705 (s), 674 (w), 658 (w), 623 (w), 610 (w). Anal. Calcd for C₅₄H₃₉NaO₃Sr· $\frac{1}{2}$ PhMe (mol wt 892.46; $\frac{1}{2}$ PhMe was lost upon exposure to vacuum): Na, 2.58; Sr, 9.80. Found: Na, 2.38; Sr, 10.60.

[KSr(Odpp)₃] (2). Sr (0.26 g, 3.0 mmol), HOdpp (0.50 g, 2.0 mmol), KOdpp (0.28 g, 1.0 mmol), and Mes*H (0.5 g, 2.0 mmol) were heated at 225 °C for 7 days. Crystalline materials were deposited on the walls of the tube, and a suitable crystal was hand-picked for crystallographic analysis. No further analysis was performed, as workup of this compound gave **3**.

[KSr(Odpp)₃]·PhMe (3). The crude product **2** was dissolved in hot PhMe (20 mL), and the solution was filtered while hot to remove excess metal. The slightly yellow solution was cooled to room temperature overnight to afford colorless crystals. Yield: 0.64 g (70%). Mp (sealed tube/N₂): 266–270 °C. ¹H NMR (300 MHz, benzene-*d*₆, 25 °C): δ 2.11 (s, 1.5H, CH₃–PhMe), 6.75 [t, 9H, *p*-H(Ph) + *p*-aryl-H], 6.86 [t, 12H, *m*-H(Ph)], 7.15 (m, 2.5H, aryl-PhMe), 7.31 (d, 6H, *m*-aryl-H), 7.42 [d, 12H, *o*-H(Ph)]. IR (Nujol) ν (cm⁻¹): 2922 (s), 2852 (s), 1954 (w), 1893 (w), 1833 (w), 1592 (m), 1553 (m), 1494 (m), 1455 (s), 1413 (s), 1378 (s), 1297 (s), 1256 (s), 1173 (m), 1155 (m), 1108 (w), 1079 (w), 1068 (m), 1025 (w), 1010 (m), 991 (w), 919 (w), 853 (s), 799 (w), 766 (s), 756 (s), 732 (m), 706 (s), 624 (w), 610 (w). Anal. Calcd for C₅₄H₃₉KO₃Sr· $\frac{1}{2}$ PhMe (mol wt 908.62; $\frac{1}{2}$ PhMe was lost upon exposure to vacuum): Sr, 9.64. Found: Sr, 9.89.

[CsSr(Odpp)₃] (4). Sr (0.26 g, 3.0 mmol), HOdpp (0.50 g, 2.0 mmol), CsOdpp (0.38 g, 1.0 mmol), and Mes*H (0.5 g, 2.0 mmol) were heated at 235 °C for 7 days. Yellow crystalline materials were hand-picked from the tube. Yield: 0.55 g (56%). Mp (sealed tube/N₂): 292–296 °C. ¹H NMR (300 MHz, benzene-*d*₆, 25 °C): δ 6.76 (t, 3H, *p*-aryl-H), 6.80 [t, 6H, *p*-H(Ph)], 6.88 [t, 12H, *m*-H(Ph)], 7.31 (d, 6H, *m*-aryl-H), 7.50 [d, 12H, *o*-H(Ph)]. IR (Nujol) ν (cm⁻¹): 2930 (s), 2844 (s), 1957 (w), 1887 (w), 1695 (w), 1636 (w), 1601 (m), 1549 (m), 1461 (s), 1415 (s), 1298 (m), 1240 (m), 1164 (w), 1146 (w), 1111 (w), 1059 (m), 1030 (w), 1000 (w), 983 (w), 907 (w), 837 (m), 802 (w), 744 (s), 715 (s), 610 (w). Anal. Calcd for C₅₄H₃₉CsO₃Sr (mol wt 956.43): Sr, 9.16. Found: Sr, 8.97.

[NaCa(Odpp)₃]·PhMe (5). Ca (0.12 g, 3.0 mmol), HOdpp (0.50 g, 2.0 mmol), NaOdpp (0.27 g, 1.0 mmol), and Mes*H (0.5 g, 2.0 mmol) were heated at 250 °C for 7 days. The crude product was dissolved in hot PhMe (30 mL), and the solution was filtered while hot to remove excess metal. Colorless crystals were deposited from the solution after it was cooled to 0 °C overnight. Yield: 0.18 g (20%).

Alternative procedure for **5**: Ca (0.08 g, 2.0 mmol), Na (0.04 g, 2.0 mmol), HOdpp (1.5 g, 6.0 mmol), and Mes*H (0.5 g, 2.0 mmol) were heated at 250 °C for 7 days. The crude product was dissolved in hot PhMe (30 mL) and then filtered, affording a clear, colorless solution. The volume of the solution was reduced to 10 mL under vacuum, and then the solution was layered with 5 mL of hexane. Colorless crystals were deposited after 2 days at room temperature. Yield: 0.23 g (13%). Mp (sealed tube/N₂): 228–230 °C. ¹H NMR (300 MHz, benzene-*d*₆, 25 °C): δ 2.11 (s, 3H, CH₃–PhMe), 6.75 [t, 6H, *p*-H(Ph)], 6.79 (t, 3H, *p*-aryl-H), 6.90 [t, 12H, *m*-H(Ph)], 7.10 (m, 5H, aryl-PhMe), 7.29 (d, 6H, *m*-aryl-H), 7.42 [d, 12H, *o*-H(Ph)]. IR (Nujol) ν (cm⁻¹): 2920 (s), 1895 (w), 1660 (w), 1592 (m), 1585 (m), 1555 (m), 1455 (s), 1411 (s), 1377 (s), 1308 (m), 1295 (m), 1259 (m), 1173 (w), 1154 (w), 1082 (m), 1069 (m), 1025 (w), 1009 (w), 919 (w), 853 (s), 800 (m), 752 (s), 727 (w), 704 (s), 665 (w), 622 (w). Anal. Calcd for C₅₄H₃₉NaO₃Ca·PhMe (mol wt 890.92): Na, 2.58; Ca, 4.50. Found: Na, 2.68; Ca, 4.87.

[KCa(Odpp)₃] (6). Ca (0.08 g, 2.0 mmol), HOdpp (0.50 g, 2.0 mmol), KOdpp (0.28 g, 1.0 mmol), and Mes*H (0.5 g, 2.0 mmol) were heated at 250 °C for 14 days. A small number of crystals were hand-picked from the crude product in the tube. ¹H NMR (300 MHz, benzene-*d*₆, 25 °C): δ 6.78 [m, 9H, *p*-H(Ph) + *p*-aryl-H], 6.90 [t, 12H, *m*-H(Ph)], 7.28 (d, 6H, *m*-aryl-H), 7.43 [d, 12H, *o*-H(Ph)]. The small amount of pure product isolated did not allow for further analysis. However, workup of this compound gave **8**.

[CsCa(Odpp)₃] (7). Ca (0.12 g, 2.0 mmol), HOdpp (0.50 g, 2.0 mmol), CsOdpp (0.38 g, 1.0 mmol), and Mes*H (0.5 g, 2.0 mmol) were heated at 235 °C for 7 days. Yellow crystalline materials were hand-picked from the tube. Yield: 0.26 g (29%). Mp (sealed tube/N₂): 275–280 °C. ¹H NMR (300 MHz, benzene-*d*₆, 25 °C): δ 6.84 [m, 21H, *p*-aryl-H + *p*-H(Ph) + *m*-H(Ph)], 7.29 (d, 6H, *m*-aryl-H), 7.51 [d, 12H, *o*-H(Ph)]. IR (Nujol) ν (cm⁻¹): 2920 (s), 2850 (s), 1596 (w), 1566 (w), 1531 (w), 1461 (s), 1409 (m), 1368 (s), 1310 (m), 1240 (w), 1176 (w), 1146 (w), 1070 (w), 1024 (w), 1000 (w), 995 (w), 855 (m), 802 (w), 744 (s), 726 (w), 697 (s), 592 (m).

[KCa(Odpp)₃(thf)]·PhMe (8). The crude product **6** was dissolved in 6:1 toluene/THF solution (35 mL), and the clear yellow solution was cooled to 0 °C. Colorless crystals were deposited after 7 days. Yield: 0.20 g (23%). Mp (sealed tube/N₂): first, 192 °C (softens); second, 237–240 °C. ¹H NMR (300 MHz, benzene-*d*₆, 25 °C): δ 1.75 (br s, 4H, CH₂-THF), 3.02 (br s, 4H, OCH₂-THF), 6.81 [m, 9H, *p*-H(Ph) + *p*-aryl-H], 6.90 [t, 12H, *m*-H(Ph)], 7.30 (d, 6H, *m*-aryl-H), 7.51 [d, 12H, *o*-H(Ph)]. IR (Nujol) ν (cm⁻¹): 2914 (s), 1952 (w), 1882 (w), 1835 (w), 1771 (w), 1677 (w), 1590 (m), 1555 (m), 1456 (s), 1111 (m), 1024 (m), 1012 (w), 919 (w), 855 (s), 808 (w), 750 (s), 703 (s), 627 (w), 598 (s). Anal. Calcd for C₅₈H₄₇KO₄Ca (mol wt 887.08; PhMe was lost upon exposure to vacuum): Ca, 4.52. Found: Ca, 4.67.

[Li₂Sr(Odpp)₄]·PhMe (9). Sr (0.26 g, 3.0 mmol), HOdpp (0.50 g, 2.0 mmol), LiOdpp (0.52 g, 2.0 mmol), and Mes*H (0.5 g, 2.0 mmol) were heated at 235 °C for 5 days. The crude product was dissolved in hot PhMe (30 mL), and the solution was filtered while hot to remove excess metal. Reducing the volume of the yellow-green solution to 15 mL and layering the solution with 5 mL of hexane afforded colorless crystals formed at room temperature after 4 days. Yield: 0.41 g (35%). Mp (sealed tube/N₂): 205–208 °C. ¹H NMR (300 MHz, benzene-*d*₆, 25 °C): δ 2.11 (s, 3H, CH₃–PhMe), 6.74 (t, 4H, *p*-aryl-H), 6.84 [t, 8H, *p*-H(Ph)], 6.96 [t, 16H, *m*-H(Ph)], 7.11 (d, 8H, *m*-aryl-H), 7.15 (m, 5H, aryl-PhMe), 7.20 [d, 16H, *o*-H(Ph)]. IR (Nujol) ν (cm⁻¹): 2920 (s), 2853 (s), 1958 (w), 1888 (w), 1818 (w), 1596 (m), 1491 (m), 1444 (s), 1409 (s), 1380 (s), 1310 (m), 1275 (m), 1257 (m), 1176 (w), 1147 (w), 1007

(27) Spek, A. L. *PLATON, A Multipurpose Crystallographic Tool*; Utrecht University: Utrecht, The Netherlands, 1998.

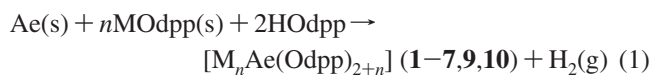
(28) Spek, A. L. *Acta Crystallogr., Sect. A* **1990**, *46*, C43.

(w), 919 (w), 849 (s), 808 (w), 750 (s), 697 (s), 604 (s). Anal. Calcd for $C_{72}H_{52}Li_2O_4Sr \cdot PhMe$: Sr, 7.46. Found: Sr, 7.85.

[Li₂Ca(Odpp)₄]·hexane (10). Ca (0.12 g, 3.0 mmol), HOdpp (0.50 g, 2.0 mmol), LiOdpp (0.26 g, 1.0 mmol), and Mes*H (0.5 g, 2.0 mmol) were heated at 235 °C for 10 days. The crude product was dissolved in hot PhMe (30 mL) to give a blue solution after stirring for 2 h. The solution was filtered while hot to remove excess metal. Reduction of the volume to 10 mL under vacuum and layering the solution with 5 mL of hexane afforded pale-blue platelike crystals deposited from the solution after cooling to 0 °C for 1 week. Repeated attempts to obtain the ¹H NMR spectrum of **10** showed only overlapping peaks in the aromatic region, thus precluding detailed analysis. Yield: 0.08 g (15%). Mp (sealed tube/N₂): 158–162 °C. IR (Nujol) ν (cm⁻¹): 2943 (s), 2844 (s), 1952 (w), 1893 (w), 1811 (w), 1666 (w), 1601 (m), 1496 (m), 1456 (s), 1403 (s), 1380 (m), 1316 (w), 1292 (s), 1257 (s), 1176 (m), 1088 (w), 1070 (m), 1018 (w), 1012 (w), 995 (w), 855 (s), 755 (s), 703 (s), 610 (s). Anal. Calcd for $C_{72}H_{52}Li_2O_4Ca$ (mol wt 1033.96; hexane was lost upon exposure to vacuum): Ca, 3.88. Found: Ca, 3.97.

Results and Discussion

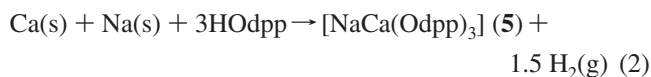
Synthetic Aspects and Solution Studies. The target compounds were prepared by reaction of elemental strontium (**1–4** and **9**) or calcium (**5–7** and **10**) with HOdpp and alkali phenolate in the flux medium MesH in an evacuated Carius tube at 225–250 °C, according to eq 1:



where for **1**, Ae = Sr, M = Na, and $n = 1$; for **2** and **3**, Ae = Sr, M = K, and $n = 1$; for **4**, Ae = Sr, M = Cs, and $n = 1$; for **5**, Ae = Ca, M = Na, and $n = 1$; for **6**, Ae = Ca, M = K, and $n = 1$; for **7**, Ae = Ca, M = Cs, and $n = 1$; for **9**, Ae = Sr, M = Li, and $n = 2$; and for **10**, Ae = Ca, M = Li, and $n = 2$. In the case of **5**, elemental sodium was also used as the source of the alkali metal. Crystalline materials of compounds **1**, **3**, **5**, **9**, and **10** were obtained by crystallization from toluene, while **2**, **4**, **6**, and **7** were isolated directly from the tube. The addition of THF to **6** afforded the adduct **8**. In accord with the trend of increasing reactivity upon descending group 2, the reactions involving calcium were slower, often requiring higher reaction temperatures than those involving the more electropositive metals strontium and barium. Typically, the lighter metals also afforded significantly lower yields than the heavier congeners.

The synthesis of the strontium-containing species **1–4** and **9** progressed as efficiently as that of the M/Ba species,¹⁹ as evidenced by the comparable yields for these two groups of compounds. Despite the relatively low reactivity of calcium, the synthetic approach used here offers an attractive route for the target compounds, as they were obtained in the absence of mercury. Activation of the metal by addition of a few drops of mercury to form a more-reactive amalgam is a necessary step in solid-state metalation of rare earth metals as well as in a few syntheses involving alkaline earth metals.^{29–31}

Interestingly, compound **5** can also be conveniently prepared using a variation of the synthetic procedure that involves mixing the bulk metals in combination with the phenol according to eq 2,



which provides a more attractive and economical strategy, as no air-sensitive aryloxides must be prepared. An analogous route was also described for the synthesis of [NaBa(Odpp)₃],¹⁹ and although it was not attempted for the strontium analogue, it is expected that this method would afford the related target compound. The formation of the series of target compounds was reproducible, with the lithium-based compounds always yielding a 2:1 M/Ae stoichiometry and the heavier alkali metal-based compounds always exhibiting a 1:1 ratio, independent of reagent stoichiometry.

The strontium species **1–4** as well as the calcium derivatives **5** and **10** showed excellent solubility in hot toluene, permitting isolation of high-purity crystal crops. Compounds **6** and **7**, which incorporate the heavier alkali metals, showed low solubility in toluene. The choice of toluene as the recrystallization solvent was based on the syntheses of the parent donor-free homometallic aryloxides [Ae₂(Odpp)₄] (Ae = Ca, Sr, Ba)³² and the aryloxolanthanoidates [Na{Nd(Odpp)₄}]³³ and [K{Ln(Odpp)₄}] (Ln = La, Nd);³⁴ we thus anticipated the formation of donor-free species of the heterobimetallic derivatives. In addition, it was possible that toluene could stabilize the metal centers through π bonding, as displayed in some heterobimetallic alkali/rare earth pyrazolate complexes.³⁵

While we were able to obtain a pure sample of **7** that was large enough for analytical characterization without further workup, the low solubility of **6** even in hot toluene posed some difficulties in its purification. For the sake of solubility, we added a small amount of the polar solvent THF to the toluene; the crude product dissolved in 6:1 toluene/THF, giving a clear, slightly yellow-colored solution. Instead of a donor-free K/Ca species, colorless crystals of the solvated species **8** were deposited from the solution upon cooling at 0 °C.

To further investigate the coordination of THF to the target compounds, treatment of **7** with a 1:1 toluene/THF solution resulted in complete dissolution of the compound. Instead of a solvated species as described in the preparation of **8**, the known homometallic polymeric compound [CsOdpp]_n deposited from the mother liquor, as confirmed by X-ray diffraction.²⁴ This result adds to those of previous studies

(30) Hitzbleck, J.; Deacon, G. B.; Ruhlandt-Senge, K. *Angew. Chem., Int. Ed.* **2004**, *43*, 5218–5220.

(31) Deacon, G. B.; Forsyth, C. M.; Harika, R.; Junk, P. C.; Ziller, J. W.; Evans, W. J. *J. Mater. Chem.* **2004**, *14*, 3144–3149.

(32) Deacon, G. B.; Forsyth, C. M.; Junk, P. C. *J. Organomet. Chem.* **2000**, *607*, 112–119.

(33) Deacon, G. B.; Feng, T.; Junk, P. C.; Skelton, B. W.; White, A. H. *J. Chem. Soc., Dalton Trans.* **1997**, 1181–1186.

(34) Deacon, G. B.; Gitlits, A.; Junk, P. C.; Skelton, B. W.; White, A. H. *Z. Anorg. Allg. Chem.* **2005**, *631*, 861–865.

(35) Deacon, G. B.; Delbridge, E. E.; Evans, D. J.; Harika, R.; Junk, P. C.; Skelton, B. W.; White, A. H. *Chem.—Eur. J.* **2004**, *10*, 1193–1204.

(29) Deacon, G. B.; Forsyth, C. M.; Gitlits, A.; Skelton, B. W.; White, A. H. *Dalton Trans.* **2004**, 1239–1247.

in our laboratory concerning the propensity of donor coordination in a family of related alkali/barium compounds.¹⁹ In this previous work, the addition of the coordinating Lewis base donors THF and diglyme {diglyme = [bis(2-methoxyethyl) ether]} to toluene solutions of [Li₂Ba(Odpp)₄] and [KBa(Odpp)₃], respectively, resulted in the solvates [Li₂(thf)₂Ba(Odpp)₄] and [KBa(Odpp)₃(diglyme)].¹⁹ These solvated heterobimetallic compounds, together with **8**, demonstrate the competition between π interactions and donation by Lewis base donors in coordination to metal centers.

These results further demonstrate that if the metal–solvent interactions become more favorable than the metal– π interactions, because of either equilibrium considerations or high metal–donor bond strengths, homometallic compounds are obtained. We can envision the solvated mixed-metal complexes (**8**, for example) as “intermediates” along the pathway for formation of the homometallic species from the heterobimetallic complexes. We anticipate that if a large amount of THF is added to **6**, a homometallic THF adduct will form. This has been demonstrated previously in the treatment of [K{Ba(Odpp)₃}] with a small amount (0.30 mL) of diglyme, resulting in [KBa(Odpp)₃(diglyme)], while addition of a 10-fold increase of the donor (3.0 mL) and using THF as the solvent resulted in the precipitation of [Ba(Odpp)₂(diglyme)₂].³⁶ Incidentally, in an attempt to synthesize a Sr/Ca compound, [Sr(Odpp)₂(thf)₃] was obtained quantitatively from a solution of the crude solid-state metalation product in 2.5:1 toluene/THF.³⁶ Although the homometallic complex was obtained in crystalline form, the possibility of heterobimetallic complexes in solution could not be ruled out; precipitation of the homometallic species may simply have indicated its reduced solubility.⁷ Conversely, formation of homometallic compounds may also explain the reduced yields for heterobimetallic compounds, although incomplete precipitation of the target compound also provides a plausible explanation. Illustrating the difference between alkaline earth and rare earth metals, addition of diglyme to a THF solution of [Na{Ln(Odpp)₃}] (Ln = Nd, Er) afforded the solvent-separated compounds [Na(diglyme)₂][Ln(Odpp)₄].³³

Our investigations of other mixed-metal systems involving group 2 metals further emphasize the role of the solvent in the formation of homometallic versus heterobimetallic compounds. For example, [Mg(Odpp)₂(donor)₂] (donor = THF, Et₂O) precipitated from the respective coordinating-donor solvents during efforts to prepare mixed Li/Mg compounds, but replacing the polar solvents with toluene in recrystallization of the product resulted in the solvated complexes [LiMg(Odpp)₃(thf)₂] and [LiMg(Odpp)(Et₂O)], respectively.⁵ Favorable formation of homometallic species in solution chemistry seems to be a recurring theme even in other heterobimetallic systems, as nearly complete recovery of [Mg(Odpp)₂(thf)₂] was observed when this compound was combined with [Ba₂(Odpp)₄] in THF, but removal of the solvent and addition of hot toluene afforded the separated-

ion Ba/Mg complex [Ba₂(Odpp)₃][Mg(Odpp)₃(thf)].³⁶ It is apparent that toluene favors the donor-free heterobimetallic species, as it does not disrupt the secondary interactions that are the major stabilization force in these compounds (see below), while the polar coordinating-donor solvents increase the tendency to form the homometallic species, frequently as their solvated derivatives. To avoid the complications brought about by solvent effects in solution chemistry, solid-state metalation is deemed to be a highly desirable synthetic approach for the preparation of heterobimetallic compounds involving alkaline earth metals. As shown in the syntheses of **4** and **7**, the target compounds can be obtained in high purity without further workup.

Room-temperature ¹H NMR spectra in C₆D₆ were obtained, and the revealed resonances were attributed to a single environment of the Odpp[−] ligand for compounds **1–9** in addition to toluene solvate or THF signals where appropriate. The spectrum of **10** showed indistinguishable, broad peaks in the aromatic region, but metal analysis confirmed the constitution of the compound. With a common 1:1 M/Ae metal ratio and structural motif (see below), compounds **1–8** had very similar aryloxo chemical shifts that differed only in the overlapping triplets representing the meta and para hydrogens in the two Cs/Ae species **4** and **7**. On the other hand, the resonances in **9**, which has a 2:1 M/Ae ratio and doubly bridging aryloxides, were located further upfield; this was particularly evident in the case of the doublets corresponding to the ortho hydrogens. Not so surprisingly, these observations are consistent with the solution-state behavior of the corresponding formulations in the family of M/Ba complexes.¹⁹ The distinct resonances of the 1:1 and 2:1 formulations among the series of Ca, Sr, and Ba compounds indicate that the solid-state features are maintained in solution. Since the aromatic NMR solvent may compete with the metal– π interactions, detection of metal– π -arene interactions in solution was precluded.

Structural Description. The solid-state structures of the series of M/Ca and M/Sr complexes can be classified into two general structural types. Compounds **1–8** represent compounds displaying a 1:1 M/Ae stoichiometry, as illustrated by the representative structures shown in Figures 1–4, while compounds **9** and **10** represent a 2:1 M/Ae ratio, as shown in Figures 5 and 6. Relevant crystal data and data collection and refinement parameters are reported in Table 2. Pertinent bond lengths and angles in **1–4**, **5–8**, and **9** and **10** are summarized in Tables 3, 4, and 5, respectively.

In compounds **1–7**, the alkali and alkaline earth metals are bridged by three aryloxo moieties, rendering a pyramidal core on both metal centers. This unusual structure is also shared by the series of complexes [M{Ba(Odpp)₃}] (M = Na, K, Cs) involving the heavier congener, barium, emphasizing the structural preferences of the heavier group 2 metals in combination with the related alkali metals (Na, K, and Cs) and the Odpp[−] ligand.¹⁹ As expected from the difference in the ionic radii of calcium, strontium, and barium (1.00, 1.18, and 1.35 Å for six-coordinate Ca²⁺, Sr²⁺, and Ba²⁺, respectively),³⁷ variation in the structural features of these complexes is evident despite the same core structures,

(36) Zuniga, M. F.; Deacon, G. B.; Ruhlandt-Senge, K. To be submitted for publication.

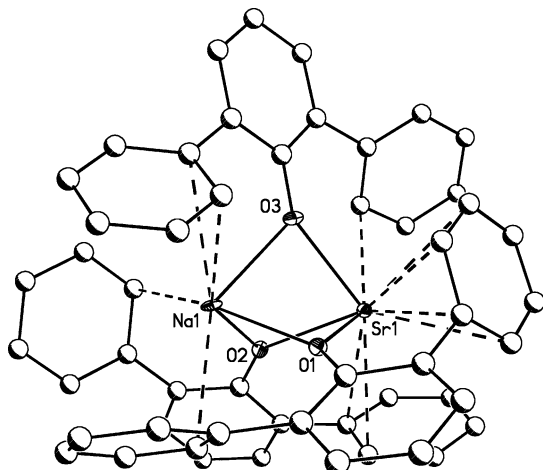


Figure 1. Structure of $[\text{NaSr}(\text{Odpp})_3] \cdot \text{PhMe}$, **1**. For clarity, hydrogen atoms and the toluene solvate molecule are not shown.

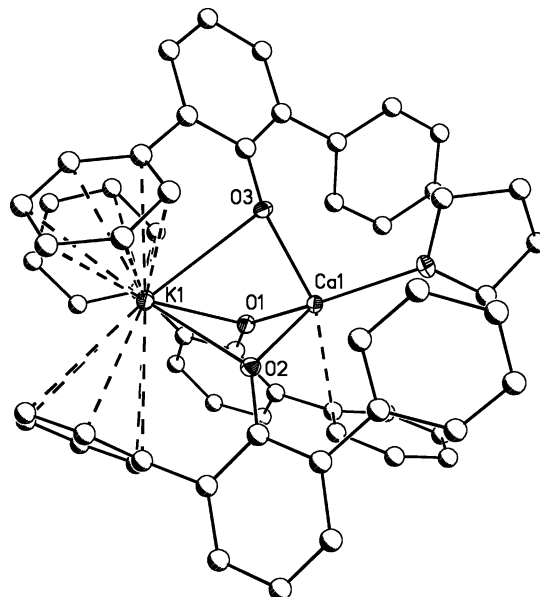


Figure 4. Structure of $[\text{KCa}(\text{Odpp})_3(\text{thf})] \cdot \text{PhMe}$, **8**. For clarity, hydrogen atoms and the toluene solvate molecule are not shown.

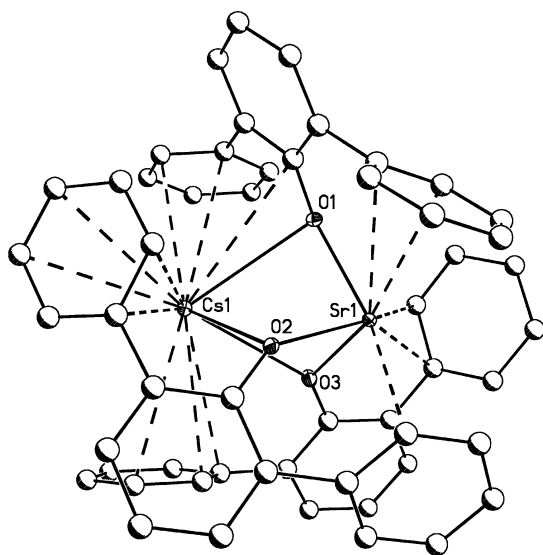


Figure 2. Structure of $[\text{CsSr}(\text{Odpp})_3]$, **4**. For clarity, hydrogen atoms are not shown.

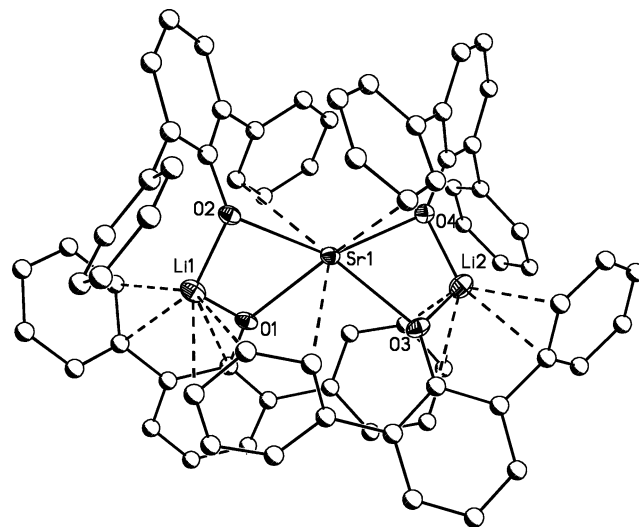


Figure 5. Structure of $[\text{Li}_2\text{Sr}(\text{Odpp})_4] \cdot \text{PhMe}$, **9**. For clarity, hydrogen atoms and the toluene solvate molecule are not shown.

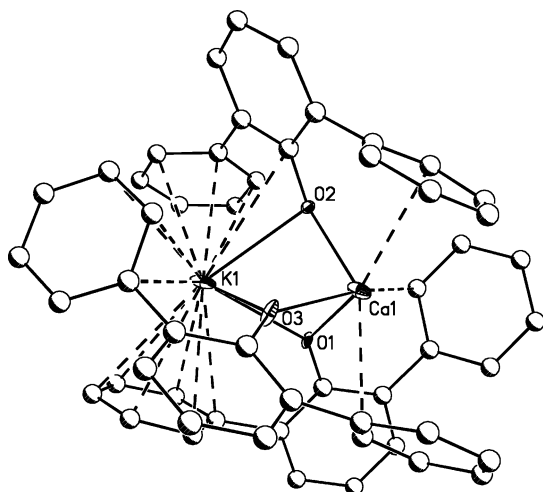


Figure 3. Structure of $[\text{KCa}(\text{Odpp})_3]$, **6**. For clarity, hydrogen atoms are not shown.

as described below. Aside from the strontium and calcium complexes reported here and the family of barium species reported earlier, other compounds involving the Odpp^- ligand

that also contain this structural motif include a family of alkali/group 14 compounds, namely, $[\text{Li}\{\text{Sn}(\text{Odpp})_3\}]^{38}$ and $[\text{M}\{\text{Ge}(\text{Odpp})_3\}]$ ($\text{M} = \text{Li}, \text{Na}, \text{K}, \text{Cs}, \text{Rb}$),³⁹ and the $[\text{Yb}_2(\text{Odpp})_3]^+$ cation.⁴⁰ The cage-like motif of compounds **1–7** is unique in comparison to the structures of several other heterobimetallic alkali calcium^{8,9} and magnesium⁴¹ complexes in which 1:1 alkali/alkaline earth metal stoichiometry is also present. As observed here, the triply bridged motif is not observed in the presence of the small lithium and magnesium ions (whose six-coordinate ionic radii are 0.76 and 0.72 Å, respectively).³⁷ Several recent examples

(37) Shannon, R. D. *Acta Crystallogr., Sect. A* **1976**, *32*, 751–767.

(38) Smith, G. D.; Fanwick, P. E.; Rothwell, I. P. *Inorg. Chem.* **1989**, *28*, 618–620.

(39) Weinert, C. S.; Fanwick, P. E.; Rothwell, I. P. *Dalton Trans.* **2003**, 1795–1802.

(40) Deacon, G. B.; Forsyth, C. M.; Junk, P. C.; Skelton, B. W.; White, A. H. *Chem.—Eur. J.* **1999**, *5*, 1452–1459.

(41) Mulvey, R. E. *Chem. Commun.* **2001**, 1049–1056.

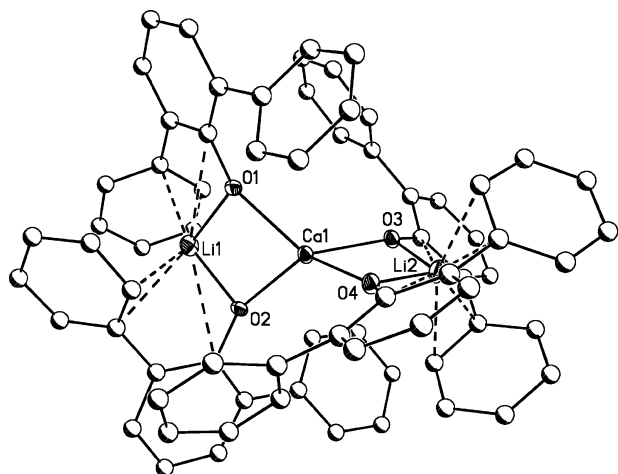


Figure 6. Structure of $[\text{Li}_2\text{Ca}(\text{Odpp})_4]\cdot\text{hexane}$, **10**. For clarity, hydrogen atoms and the hexane solvate molecule are not shown.

of magnesiates containing the Odpp^- ligand prepared in our laboratory further support this view.⁵ Consequently, compounds **1–7** offer simple molecular architectures for heterobimetallic species consisting of alkali metals in combination with heavy alkaline earth metals.

The Sr–O distances in **1** (Figure 1, Table 3) fall within a narrow range [av 2.39(2) Å] and are slightly shorter than those involving the three-(oxygen)-coordinate strontium in $[\text{Sr}_2(\mu\text{-Odpp})_3(\text{Odpp})]$ [av 2.440(6) Å]³² and the Sr–(μ -O) bond lengths [2.404(7)–2.495(7) Å] involving the hexacoordinate strontium in $[\text{Sr}_4(\text{OPh})_8(\text{PhOH})_2(\text{thf})_6]$.⁴² The Na–O bond lengths in **1** fall in a relatively wide range [2.327(2)–2.478(2) Å], in contrast to those in $[\text{Na}\{\text{Ba}(\text{Odpp})_3\}]$ [av 2.333(2) Å],¹⁹ perhaps because of the higher formal coordination number in **1**; however, they are generally shorter than those in the corresponding complex $[\text{Na}\{\text{Nd}(\text{Odpp})_4\}]$ [2.343(6)–2.722(5) Å],³³ where the sodium metal displays a higher formal coordination number than in **1**. While the O–Sr–O angles are nearly identical, the O–Na–O and Sr–O–Na angles display slight variations (3°) from each other, which may account for the differences in the Na–O bond distances or vice versa.

Employing the heavier alkali metal potassium gave two forms of the heterobimetallic K/Sr compounds. One of these (**2**) contains no solvent of crystallization, and the other (**3**) hosts a toluene molecule in the lattice that does not have any close contacts with the metal centers. Although similar structural features for **2** and **3** would be expected, close inspection of the two compounds reveals significant disparities in their solid-state structures. One critical difference is the 50:50 metal disorder exhibited in **3**, which was not observed in **2**. The disorder is unexpected for **3**, considering the significant differences in the ionic radii of potassium and strontium (1.38 and 1.18 Å for six-coordinate K^+ and Sr^{2+} , respectively).³⁷ A similar 50:50 metal disorder was previously observed for $[\text{K}\{\text{Ba}(\text{Odpp})_3\}]$ ¹⁹ but rationalized in terms of the similar ionic radii of hexacoordinate barium (1.35 Å) and potassium (1.38 Å).³⁷

The Sr–O bond lengths in both **2** [av 2.375(9) Å] and **3** [av 2.408(9) Å] are comparable to the ones in **1**, but the distances in **3** lie in a narrower range. Another evident difference between **2** and **3** is in their K–O bond lengths: these distances in **3** [av 2.617(9) Å] are significantly longer (0.30 Å) than the corresponding distances in **2** [2.362(9) Å]. The K–O distances in **3** are more comparable to those in $[\text{K}\{\text{Ba}(\text{Odpp})_3\}]$ ¹⁹ and the K–OSiPh₃ distances in $[\text{KBa}_2(\text{OSiPh}_3)_5(\text{dme})_2]$.⁴³ In comparison, the K–O distances in **2** are unusually short; the shortest [2.306(3) Å] is similar to some of the Na–O bond lengths in **1**. There are no significant differences between the Sr–O1–K angles of **2** and **3**, although a wider range for the O–Sr–O and O–K–O angles as well as the Sr–O–C and K–O–C angles is observed for **2**. The relatively broad ranges of the K–O bond distances in **2** and **3** (~0.10 and ~0.17 Å, respectively) agree with the trend due to structural flexibility and metal– π interactions (see below) that was previously established for the barium derivatives.

This disparity in M–O distances was previously observed in alkali/rare earth metal species, such as $[\text{K}\{\text{Ln}(\text{Odpp})_4\}]$ (Ln = La, Nd),³⁴ $[\text{Na}\{\text{Nd}(\text{Odpp})_4\}]$,³³ and $[\text{K}\{\text{Sm}(\text{OAr})_3(\text{thf})\}]_n$ (OAr = 2,6-*t*Bu₂-4-Me-C₆H₂O).⁴⁴ In further support of the trend of asymmetric metal–oxygen distances, the Cs–O bond lengths in **4** (Figure 2) span the range 2.913(2)–3.266(2) Å. Likewise, the presence of the large alkali metal atom in **4** led to wider O–Sr–O angles as well as an extensive array of wider Sr–O–Cs, Sr–O–C, and Cs–O–C angles.

By analogy with the strontium complexes **1–4**, heterobimetallic complexes of calcium involving the alkali metals sodium (**5**), potassium (**6**), and cesium (**7**) also exhibit the $\text{M}(\text{OR})_3\text{Ae}$ core. Interestingly, the similar structures of these families of heterobimetallic complexes contrast with the solid-state structures of the related homometallic dimeric compounds of the two metals: $[\text{Ca}_2(\mu\text{-Odpp})_2(\text{Odpp})_2]$ has two bridging and two terminal ligands, while $[\text{Ae}_2(\mu\text{-Odpp})_3(\text{Odpp})]$ (Ae = Sr, Ba) complexes contain three bridging and one terminal ligand.³² Compound **5** demonstrates a 70:30 disorder over the metal sites, which can be rationalized in terms of the similarities in their ionic radii (1.14 and 1.16 Å for six-coordinate Ca^{2+} and Na^+ , respectively). Consequently, the Ca–O and Na–O bond distances vary by as much as 0.13 Å (Table 4). In the case of the heavier alkali metals, the Ca–O bond lengths in **6** [2.215(4)–2.246(5) Å] and **7** [2.168(1)–2.198(1) Å] both span a narrow range and are slightly shorter than the bridging distances in dimeric $[\text{Ca}_2(\mu\text{-Odpp})_2(\text{Odpp})_2]$ [2.249(2)–2.275(2) Å]³² as well as in $[\text{Ca}_2(\mu\text{-ciox})_2(\text{ciox})_2(\text{thf})_2]$ [ciox = OC(C₆H₅)₂CH₂-*p*-C₆H₄Cl] [2.268(2) and 2.299(2) Å],⁴⁵ possibly as a result of the higher coordination of the calcium atoms in the latter complexes. The K–O bond

(42) Drake, S. R.; Streib, W. E.; Chisholm, M. H.; Caulton, K. G. *Inorg. Chem.* **1990**, *29*, 2707–2708.

(43) Coan, P. S.; Streib, W. E.; Caulton, K. G. *Inorg. Chem.* **1991**, *30*, 5019–5023.

(44) Evans, W. J.; Anwender, R.; Ansari, M. A.; Ziller, J. W. *Inorg. Chem.* **1995**, *34*, 5–6.

(45) Tesh, K. F.; Hanusa, T. P.; Huffman, J. C.; Huffman, C. J. *Inorg. Chem.* **1992**, *31*, 5572–5579.

Table 2. Crystallographic Data for Compounds **1–10**

	1	2	3	4	5
formula	C ₆₁ H ₄₇ NaSrO ₃	C ₅₄ H ₃₉ KSrO ₃	C ₆₁ H ₄₇ KSrO ₃	C ₅₄ H ₃₉ CsSrO ₃	C ₆₁ H ₄₇ CaNaO ₃
fw	938.46	862.57	954.57	956.38	890.92
<i>a</i> (Å)	15.2863(7)	17.855(2)	15.509(1)	39.063(4)	15.054(1)
<i>b</i> (Å)	16.6856(8)	11.956(1)	16.567(2)	10.806(1)	17.078(2)
<i>c</i> (Å)	18.3924(8)	19.238(2)	18.553(2)	21.184(2)	18.197(2)
α (deg)	90	90	90	90	90
β (deg)	94.201(1)	91.352(2)	94.770(2)	109.835(2)	92.291(2)
γ (deg)	90	90	90	90	90
<i>V</i> (Å ³)	4678.6(4)	4105.6(6)	4750.4(7)	8412(1)	4674.4(8)
<i>Z</i>	4	4	4	8	4
space group	<i>P</i> 2 ₁ / <i>c</i>	<i>P</i> 2 ₁ / <i>c</i>	<i>P</i> 2 ₁ / <i>c</i>	<i>C</i> 2/ <i>c</i>	<i>P</i> 2 ₁ / <i>c</i>
<i>d</i> _{calc} (g/cm ³)	1.202	1.395	1.206	1.510	1.135
linear abs coeff (mm ⁻¹)	1.202	1.461	1.262	2.180	0.184
<i>T</i> (K)	92(2)	96(2)	95(2)	94(2)	93(2)
2θ range (deg)	2.68–56.66	4.02–50.0	3.60–50.0	3.92–56.68	3.28–50.0
no. of indep. reflns	11633	33077	8351	10406	8226
no. of parameters	532	532	532	532	528
R1, wR2 (all data)	0.0569, 0.1394	0.0688, 0.1499	0.0652, 0.1916	0.0453, 0.0723	0.0731, 0.1484
R1, wR2 (>2σ)	0.0484, 0.1353	0.0494, 0.1377	0.0588, 0.1866	0.0314, 0.0676	0.0570, 0.1396

	6	7	8	9	10
formula	C ₅₄ H ₃₉ CaKO ₃	C ₅₄ H ₃₉ CaCsO ₃	C ₆₅ H ₅₅ CaKO ₄	C ₁₅₁ H ₁₁₂ Li ₄ Sr ₂ O ₈	C ₇₈ H ₆₆ CaLi ₂ O ₄
fw	815.03	908.84	979.27	2257.41	1121.1
<i>a</i> (Å)	18.8914(7)	38.916(4)	16.860(3)	19.006(3)	18.503(5)
<i>b</i> (Å)	11.7985(4)	10.711(1)	12.498(2)	21.776(3)	18.542(5)
<i>c</i> (Å)	19.0598(7)	21.330(2)	25.019(4)	28.838(4)	17.301(5)
α (deg)	90	90	90	90	90
β (deg)	104.593(1)	109.891(2)	107.108(3)	103.835(3)	105.869(6)
γ (deg)	90	90	90	90	90
<i>V</i> (Å ³)	4111.2(3)	8360(2)	5038(2)	11589(3)	5710(3)
<i>Z</i>	4	8	4	4	4
space group	<i>P</i> 2 ₁ / <i>c</i>	<i>C</i> 2/ <i>c</i>	<i>P</i> 2 ₁ / <i>c</i>	<i>P</i> 2 ₁ / <i>n</i>	<i>P</i> 2 ₁ / <i>c</i>
<i>d</i> _{calc} (g/cm ³)	1.317	1.444	1.291	1.294	1.204
linear abs coeff (mm ⁻¹)	0.300	1.054	0.258	0.983	0.160
<i>T</i> (K)	99(2)	94(2)	97(2)	92(2)	83(2)
2θ range (deg)	4.10–50.00	3.92–56.78	3.40–50.0	2.90–56.82	3.18–50.0
no. of indep. reflns	7236	10440	8854	29013	10060
no. of parameters	555	532	650	1486	712
R1, wR2 (all data)	0.1353, 0.2495	0.0316, 0.0692	0.0731, 0.1323	0.0882, 0.1092	0.1472, 0.1619
R1, wR2 (>2σ)	0.1272, 0.2447	0.0279, 0.0673	0.0593, 0.1266	0.0474, 0.0982	0.0686, 0.1362

Table 3. Selected Bond Lengths (Å) and Angles (deg) in Compounds **1–4**

	[NaSr(Odpp) ₃]• PhMe, 1 (M = Na)	[KSr(Odpp) ₃], 2 (M = K)	[KSr(Odpp) ₃]• PhMe, 3 (M = K)	[CsSr(Odpp) ₃], 4 (M = Cs)
Bond Lengths				
Sr1–O1	2.380(2)	2.370(3)	2.403(3)	2.343(2)
Sr1–O2	2.410(2)	2.419(3)	2.403(3)	2.328(2)
Sr1–O3	2.387(2)	2.336(3)	2.417(3)	2.366(2)
M1–O1	2.357(2)	2.375(3)	2.559(3)	3.194(2)
M1–O2	2.327(2)	2.306(3)	2.727(3)	3.266(2)
M1–O3	2.478(2)	2.405(3)	2.564(3)	2.913(2)
Bond Angles				
O1–Sr1–O2	78.29(6)	78.40(9)	81.3(1)	89.18(5)
O1–Sr1–O3	78.46(6)	80.2(1)	82.3(1)	89.72(6)
O2–Sr1–O3	77.10(6)	73.71(9)	81.1(1)	85.67(6)
O1–M1–O2	80.42(7)	80.6(1)	72.57(9)	60.99(4)
O1–M1–O3	77.12(6)	78.7(1)	76.54(9)	65.70(4)
O2–M1–O3	76.90(7)	74.5(1)	72.54(9)	61.86(4)
Sr1–O1–M1	87.64(6)	86.96(9)	88.41(9)	87.72(5)
Sr1–O2–M1	87.62(6)	87.40(9)	84.62(8)	86.25(5)
Sr1–O3–M1	84.76(6)	87.03(9)	88.00(9)	94.20(5)
Sr1–O1–C11	134.3(2)	141.6(3)	134.2(2)	138.9(2)
Sr1–O2–C21	137.6(2)	114.8(2)	149.9(3)	147.1(1)
Sr1–O3–C31	149.2(2)	141.1(2)	138.7(2)	131.3(1)
M1–O1–C11	137.8(2)	131.4(3)	137.0(2)	106.8(1)
M1–O2–C21	133.2(2)	138.4(2)	125.3(3)	106.9(1)
M1–O3–C31	126.0(2)	121.7(2)	130.3(2)	134.5(1)

lengths [av 2.68(2) Å] in **6** (Figure 3) are slightly longer than those in **3** [av 2.617(9) Å] and in [KBa(Odpp)₃] [av 2.63(2) Å],¹⁹ a fact for which the greater degree of

metal–arene interactions in **6** than in the strontium and barium compounds (see below) may account. In addition, the O–K–O angles in **6** [av 68.8(1)°] are narrower than

Table 4. Selected Bond Lengths (Å) and Angles (deg) in Compounds **5–8**

	[NaCa(Odpp) ₃], 5 (M = Na)	[KCa(Odpp) ₃], 6 (M = K)	[CsCa(Odpp) ₃], 7 (M = Cs)	[KCa(Odpp) ₃ (thf)]· PhMe, 8 (M = K)
Bond Lengths				
Ca1–O1	2.236(2)	2.246(5)	2.168(1)	2.212(2)
Ca1–O2	2.260(2)	2.215(4)	2.189(1)	2.242(2)
Ca1–O3	2.253(2)	2.219(5)	2.198(1)	2.152(2)
Ca1–O(thf)				2.345(2)
M1–O1	2.297(2)	2.610(5)	3.318(1)	2.712(2)
M1–O2	2.362(2)	2.705(5)	3.191(1)	2.780(2)
M1–O3	2.302(2)	2.736(5)	2.948(1)	2.951(2)
Bond Angles				
O1–Ca1–O2	82.21(7)	82.2(2)	94.11(5)	90.92(7)
O1–Ca1–O3	83.09(7)	86.6(2)	90.46(5)	87.82(7)
O2–Ca1–O3	81.67(7)	88.9(2)	94.11(5)	96.16(7)
O1–Ca1–O4				144.41(8)
O2–Ca1–O4				122.94(7)
O3–Ca1–O4				98.01(7)
O1–M1–O2	78.75(6)	67.0(1)	58.64(3)	70.65(6)
O1–M1–O3	80.69(7)	69.8(1)	58.94(3)	64.46(5)
O2–M1–O3	78.47(7)	69.6(1)	62.93(3)	69.51(5)
Ca1–O1–M1	83.88(6)	88.8(1)	83.75(4)	85.98(6)
Ca1–O2–M1	81.88(6)	87.1(2)	86.58(4)	83.81(6)
Ca1–O3–M1	83.37(6)	86.2(1)	92.76(4)	81.23(6)
Ca1–O1–C11	138.4(2)	130.5(4)	146.9(1)	149.5(2)
Ca1–O2–C21	147.0(2)	138.1(4)	137.6(1)	129.5(2)
Ca1–O3–C31	139.7(2)	143.1(4)	135.8(1)	158.2(2)
M1–O1–C11	137.5(2)	137.8(4)	106.2(1)	121.3(2)
M1–O2–C21	131.0(2)	107.4(4)	107.44(9)	131.1(2)
M1–O3–C31	136.3(2)	128.8(4)	131.2(1)	110.7(2)

Table 5. Selected Bond Lengths (Å) and Angles (deg) in Compounds **9** and **10**

	[Li ₂ Sr(Odpp) ₄]·PhMe, 9 (Ae = Sr)		[Li ₂ Ca(Odpp) ₄]· hexane, 10 (Ae = Ca)
	molecule A	molecule B	
Bond Lengths			
Ae1–O1	2.463(1)	2.479(2)	2.224(2)
Ae1–O2	2.530(2)	2.479(1)	2.267(2)
Ae1–O3	2.464(1)	2.494(1)	2.217(1)
Ae1–O4	2.514(1)	2.469(1)	2.249(2)
Li1–O1	1.885(4)	1.828(4)	1.884(4)
Li1–O2	1.838(4)	1.864(4)	1.859(4)
Li2–O3	1.877(5)	1.822(4)	1.904(4)
Li2–O4	1.819(4)	1.873(4)	1.866(4)
Bond Angles			
O1–Ae1–O2	72.52(5)	69.90(5)	78.84(6)
O1–Ae1–O3	105.24(5)	133.33(5)	119.20(6)
O1–Ae1–O4	138.03(5)	139.91(5)	136.48(6)
O2–Ae1–O3	139.62(5)	144.41(5)	119.13(6)
O2–Ae1–O4	138.14(5)	110.53(5)	129.28(6)
O3–Ae1–O4	70.26(5)	70.44(5)	79.10(5)
O1–Li1–O2	105.0(2)	100.6(2)	99.3(2)
O3–Li2–O4	101.6(2)	101.5(2)	97.9(2)
Ae1–O1–Li1	89.0(1)	91.3(1)	91.3(1)
Ae1–O2–Li1	88.0(1)	90.4(1)	90.6(1)
Ae1–O3–Li2	91.1(1)	91.2(1)	91.2(1)
Ae1–O4–Li2	90.9(2)	90.8(1)	91.2(1)
Ae1–O1–C11	149.6(1)	132.8(1)	155.4(1)
Ae1–O2–C21	131.2(1)	148.5(1)	149.1(1)
Ae1–O3–C31	145.9(2)	137.2(1)	149.5(1)
Ae1–O4–C41	134.2(1)	145.5(1)	150.9(1)
Li1–O1–C11	119.7(2)	130.3(2)	113.3(2)
Li1–O2–C21	134.8(2)	119.7(2)	114.9(2)
Li2–O3–C31	118.2(2)	127.0(2)	113.3(2)
Li2–O4–C41	130.9(2)	118.1(2)	116.8(2)

those in the heavier analogues {av 73.9(3) and 73.6(6)^o in **3** and [KBa(Odpp)₃], respectively}.¹⁹ As a reflection of the large size of the alkali metal atom, the Cs–O bond lengths in **7** [2.948(1)–3.318(1) Å], which vary by as much as 0.37 Å, are comparable to the ones in **4**. These

values are also associated with a wide range of Ca–O–Cs angles [83.75(4)–92.76(4)^o].

Addition of THF to **6** afforded [KCa(Odpp)₃(thf)]·PhMe, **8** (Figure 4), in which the donor coordinates to the calcium center. This results in a distorted tetrahedral environment around the Ca atom, with the O–Ca–O angles involving the three bridging aryloxides ranging from 87.82(7) to 96.16(7)^o and the O(Ar)–Ca–O(thf) angles in the range 98.01(7)–144.41(8)^o. The triply bridged nature of the metals is retained, while extensive K– π -phenyl interactions are evident. By way of comparison, in the solvated heterobimetallic species previously obtained by our group, thf coordinated to each of the lithium centers in [Li₂(thf)₂Ba(Odpp)₄] while diglyme preferentially coordinated to the barium center in [KBa(Odpp)₃(diglyme)].¹⁹ The preferred coordination of thf to calcium versus potassium was previously noted in the K/Ca enolate complex [K₂(thf)₂Ca₂{OC(Mes)=CH₂}₆] and was attributed to the higher Lewis acidity of calcium compared with potassium.¹⁰ Previous solvated amido calcates, for example, [LiCa{N(SiMe₃)₂}₃(thf)]⁹ and [KCa{N(SiMe₃)₂}₃(thf)]_∞,¹⁰ exhibit a different solvation mode, with coordination of the Lewis base donor to the alkali metals, perhaps as a result of steric effects.

Despite the increased coordination number of calcium in **8**, two of the Ca–O(Ar) bond lengths in this compound compare well to those in **5–7**. The Ca–O3(Ar) bond [2.152(2) Å in **8**] is unusually short for a Ca– μ -O interaction, and its length is nearly equal to the terminal Ca–O distances in [Ca₂(μ -Odpp)₂(Odpp)₂] [2.122(2) and 2.120(2) Å].³² The shortening of the Ca–O3 bond is compensated by the lengthening of the corresponding K–O3 bond [2.951(2) Å], while the other two K–O bond lengths [2.712(2) and 2.780(2) Å] are comparable to those in [K{Ba-

Table 6. Metal–Carbon Distances d (Å) for Metal– π -Phenyl Interactions in **1–10**^a

1 (Na, Sr)		2 (K, Sr)		3 (K, Sr)		4 (Cs, Sr)		5 (Na, Ca)		6 (K, Ca)	
<i>n</i>	<i>d</i>	<i>n</i>	<i>d</i>	<i>n</i>	<i>d</i>	<i>n</i>	<i>d</i>	<i>n</i>	<i>d</i>	<i>n</i>	<i>d</i>
Sr1–C _{<i>n</i>}		Sr1–C _{<i>n</i>}		Sr1–C _{<i>n</i>}		Sr1–C _{<i>n</i>}		Ca1–C _{<i>n</i>}		Ca1–C _{<i>n</i>}	
161	3.100(2)	162	3.128(4)	161	3.135(3)	162	3.017(2)	162	2.865(3)	162	3.010(6)
162	3.310(3)	21	3.196(4)	162	3.074(4)	266	3.101(2)	266	2.984(3)	266	2.912(6)
165	3.185(2)	261	3.105(4)	163	3.222(4)	361	3.157(2)	362	2.927(3)	366	3.045(8)
166	3.051(2)	262	3.278(4)	266	3.172(4)	366	3.127(3)				
221	3.170(2)	361	3.142(4)	361	3.236(4)			Na1–C _{<i>n</i>}			
222	3.070(2)	362	3.254(4)	362	3.154(4)	Cs–C _{<i>n</i>}		126	2.846(2)	K1–C _{<i>n</i>}	
326	3.099(3)	363	3.292(4)			11	3.785(2)	226	2.839(3)	121	3.249(7)
		364	3.240(4)	K1–C _{<i>n</i>}		121	3.491(2)	326	2.898(3)	122	3.424(7)
Na1–C _{<i>n</i>}		365	3.165(5)	121	3.474(4)	122	3.539(2)			123	3.499(7)
126	2.926(3)	366	3.102(4)	122	3.083(4)	221	3.439(2)			124	3.413(7)
262	2.936(3)			123	3.444(4)	222	3.567(2)			125	3.229(7)
361	3.037(2)	K1–C _{<i>n</i>}		221	3.125(4)	223	3.798(2)			126	3.192(6)
366	2.786(2)	11	3.391(4)	222	3.020(4)	224	3.802(2)			21	3.334(6)
		121	3.191(4)	223	3.296(4)	226	3.572(2)			221	3.194(6)
		125	3.390(4)	226	3.446(4)	321	3.675(2)			222	3.483(6)
		126	2.887(4)	321	3.282(4)	325	3.647(2)			226	3.494(6)
		21	3.396(4)	322	3.131(4)	326	3.469(2)			321	3.391(6)
		221	3.192(4)	323	3.397(4)					325	3.473(6)
		225	3.069(5)							326	3.155(6)
		226	2.775(4)								
		31	3.291(4)								
		321	3.270(4)								
		322	3.070(4)								
7 (Cs, Ca)		8 (K, Ca)		9A (Li ₂ , Sr)		9B (Li ₂ , Sr)		10 (Li ₂ , Ca)			
<i>n</i>	<i>d</i>	<i>n</i>	<i>d</i>	<i>n</i>	<i>d</i>	<i>n</i>	<i>d</i>	<i>n</i>	<i>d</i>		
Ca1–C _{<i>n</i>}		Ca1–C _{<i>n</i>}		Sr1–C _{<i>n</i>}		Sr1–C _{<i>n</i>}		Ca1–C _{<i>n</i>}			
166	2.998(2)	126	2.997(3)	266	3.234(2)	566	3.196(2)	no close contacts			
266	2.916(2)			326	3.246(2)	666	3.205(2)				
362	3.022(2)	K1–C _{<i>n</i>}		426	3.214(2)	726	3.236(2)	Li1–C _{<i>n</i>}			
		161	3.213(3)			822	3.244(2)	11	2.709(8)		
Cs1–C _{<i>n</i>}		165	3.495(3)	Li1–C _{<i>n</i>}				161	2.376(7)		
121	3.455(2)	166	3.160(3)	11	2.798(4)	Li3–C _{<i>n</i>}		162	2.418(7)		
122	3.560(2)	261	3.181(3)	121	2.555(4)	61	2.770(4)	21	2.725(8)		
123	3.765(2)	262	3.384(3)	126	2.664(4)	621	2.594(4)	261	2.589(8)		
125	3.787(2)	263	3.521(3)	324	2.691(5)	626	2.677(5)	266	2.423(8)		
126	3.581(2)	264	3.466(3)	325	2.705(5)	823	2.680(5)				
21	3.797(2)	265	3.228(3)			824	2.712(5)	Li2–C _{<i>n</i>}			
221	3.514(2)	266	3.078(3)	Li2–C _{<i>n</i>}				31	2.729(8)		
222	3.523(2)	361	3.099(3)	164	2.838(5)	Li4–C _{<i>n</i>}		321	2.394(8)		
321	3.599(2)	362	3.220(3)	165	2.643(5)	665	2.772(5)	326	2.504(9)		
325	3.622(2)	363	3.432(3)	31	2.761(5)	71	2.830(5)	41	2.748(8)		
326	3.467(2)	364	3.519(3)	361	2.572(5)	81	2.757(4)	421	2.531(9)		
		365	3.411(3)	362	2.675(5)	861	2.575(4)	426	2.403(9)		
		366	3.205(3)			866	2.586(5)				

^a Each carbon atom with a two-digit label ($n = xy$) takes part in a metal–ligand interaction involving a ligand phenoxy ring: x indicates the oxygen number of the aryloxy ligand and y indicates the number of the carbon within the phenoxy ring that interacts with M or Ae. Each carbon atom with a three-digit label ($n = xyz$) takes part in a metal–ligand interaction involving a ligand phenyl substituent: x indicates the oxygen number of the aryloxy ligand, y indicates the position (2 or 6) of the phenyl substituent, and z indicates the number of the carbon within the phenyl ring that interacts with M or Ae.

(Odp)₃(diglyme)}] [av 2.779(6) Å].¹⁹ Nevertheless, all three of the K–O bond lengths are within the range of significant bridging distances in [K{Sm(OAr)₃(thf)}]_{*n*} [2.778(6) and 2.967(9) Å].⁴⁴ These observations are supported by the proximity of thf to O3, with an O3–Ca–O(thf) angle of 98.02(8)°, as opposed to the other two aryloxy moieties, with O1,2–Ca–O(thf) angles of 122.96(8) and 144.42(8)°, respectively. In comparison with the Ca–O(Ar) distance in the donor-free species **6**, shorter bond lengths are observed

in **8**, which is contrary to the expected lengthening of the bond distances due to increased oxygen coordination. This discrepancy may be explained by the smaller degree of calcium–arene interactions as well as reduced steric influence from the phenyl rings in **8**, allowing shorter Ca–O(Ar) bond lengths. On the other hand, the Ca–O(thf) distance [2.344(2) Å] is considerably longer than the lengths of the bridging Ca–O(Ar) bonds in both **6** and **8** but is comparable to the Ca–O(thf) distances in previously reported heterobi-

metallic enolate complexes, one involving a pentacoordinate calcium, $[\text{K}_2\text{Ca}_2\{\text{OC}(\text{Mes})=\text{CH}_2\}_6(\text{thf})_2]$ [2.406(2) Å], and the other a hexacoordinate calcium, $[\text{K}_2\text{Ca}\{\text{OC}(\text{Mes})=\text{CH}_2\}_4(\text{thf})_4]$ [2.297(5) Å].¹⁰ Moreover, compound **8** displays longer K–O bond distances [2.712(2)–2.951(2) Å] in comparison with **6**. The coordination of thf to the calcium center causes the phenyls to orient toward the potassium metal, consequently increasing the number of close contacts with the phenyl substituent (see below).

Employing the alkali metal lithium afforded compounds **9** (Figure 5) and **10** (Figure 6), both of which contain a 2:1 Li/Ae (Ae = Sr, Ca) ratio. In these compounds, the metal centers are bridged by two pairs of aryloxo ligands, resulting in a core that consists of two fused four-membered rings, each composed of the alkaline earth metal, two oxygens, and one lithium metal. The four aryloxides surrounding the strontium or calcium are arranged in a distorted tetrahedral fashion, with narrow O–Ae–O angles involving the alkaline earth metal and two bridging oxygens that are linked to the same lithium center. In contrast to the cagelike structure common in the sodium, potassium, and cesium analogues, compounds **9** and **10** adopt a structural motif that is typical of mixed-metal systems involving lithium, as exemplified by $[\text{Li}_2\{\text{Ba}(\text{Odp})_4\}]$ as well as several alkali magnesiate involving alkyl, aryl, amide, enolate, or aryloxo ligands.^{5,41,46} It is important to note that for lithium in combination with the significantly smaller group 14 metals, the complexes $[\text{Li}\{\text{E}(\text{Odp})_3\}]$ (E = Ge, Sn) bear a triply bridged cagelike motif.^{38,39}

The 2:1 lithium/alkaline earth metal stoichiometry and the simple, donor-free molecular architectures of **9** and **10** differ strikingly from those previously reported for Li/Ae heterobimetallics in the presence of oxygen-based donors, for example, $[\{\text{Li}_3\text{Ba}_6\text{O}_2\}(\text{OtBu})_{11}(\text{thf})_3]$,¹⁷ $[\{\text{Li}(\text{thf})_4\}_4\text{M}(\text{OtBu})_4(\text{OH})\text{I}]$ (M = Ca, Sr, Ba),^{11–14} $[\text{Li}(\text{thf})_4][\{\text{Sr}_6(\text{OtBu})_7(\mu_3\text{-I})(\text{I})_2(\text{thf})_3\}_2(\mu\text{-I})]$,¹⁶ $[\text{Li}\{\text{Ca}_7(\mu_3\text{-OH})_8\text{I}_6(\text{thf})_{12}\}_2(\mu\text{-I})]$,⁴⁷ and $[\text{Li}_6\text{M}(\text{OPh})_8(\text{thf})_6]$ (M = Ca, Sr, Ba),^{13,15} which are based on multinuclear arrangements; however, the DME-solvated aryloxo $[\{\text{Li}(\text{dme})\}_2\text{Ca}_2(\mu\text{-OPh})_6(\text{dme})_2]$ ¹⁵ bears a good resemblance to the fused four-membered-ring core of **10**, despite its 1:1 Li/Ca ratio.

The asymmetric unit of compound **9** displays two independent molecules (**9A** and **9B**) that have quite similar geometrical features (Table 5). As expected for the increased coordination of strontium in **9** as compared with **1–4**, the Sr–O bond lengths [av 2.493(2) and 2.480(2) Å in **9A** and **9B**, respectively] are ~0.1 Å longer than those in compounds **1–4** but closely resemble the bridging distances of the tetracoordinate strontium metal in $[\text{Sr}_2(\mu\text{-Odp})_3(\text{Odp})]$.³² Similarly, the Li–O bond distances lie in a narrow range [av 1.855(4) and 1.847(4) Å in **9A** and **9B**, respectively] that falls within the distance range in $[\text{Li}_2\{\text{Ba}(\text{Odp})_4\}]$ [av 1.84(1) Å]¹⁹ but are slightly shorter than the ones in the magnesiate $[\text{Li}_2\text{Mg}(\text{OAr})_2(\text{donor})_n]$ (OAr = 2,4,6-Me₃C₆H₂O, donor = thf, *n* = 4; OAr = 3,5-*t*Bu₂C₆H₃O, donor = tmeda, *n* = 2).⁵

Conversely, the increase in the coordination number of the calcium center in **10** has no effect on the Ca–O bond distances [av 2.239(7) Å]. They are comparable to the corresponding bond lengths in **5** and **6** and are slightly longer than the ones in **7**. The close interaction of calcium with the aryloxo ligands can be rationalized in terms of the lack of secondary interactions between the metal center and the phenyl rings in **10** as opposed to the strontium (see below) and barium analogues.¹⁹ As a result of the significant steric requirement of the ligands, the fused four-membered Li₂O₂Ca rings in **10** are tilted away from each other, oriented almost orthogonally (tilt angle 88°) with a slightly nonlinear Li–Ca–Li arrangement (168°). This orientation of the rings is also observed in the related strontium and barium complexes, but the tilt angles are substantially smaller (62 and 53°, respectively) as explained by decreased steric strain due to the increased metal–ligand bond lengths. Likewise, the Li–Ae–Li angles are smaller (156 and 153° for Ae = Sr and Ba, respectively), an orientation necessary to maximize intramolecular π interactions for the larger metals.¹⁹ Both of the four-membered rings in **10** are planar (sum of the endocyclic angles = 360°), in contrast to the slightly puckered geometries in **9** (355 and 354°) and $[\text{Li}_2\{\text{Ba}(\text{Odp})_4\}]$ (354 and 351°).¹⁹

Demonstrating a vital stabilization force that is increasingly recognized in alkaline earth metal chemistry, compounds **1–10** reveal extensive metal– π -arene interactions involving the neutral phenyl substituents as well as the phenoxide units, as summarized in Table 6. In general, the extent of metal– π -arene interactions increases as the metal size increases, a trend established in the series of alkali/barium complexes¹⁹ as well as in alkali/germanium compounds.³⁹ In **1–7**, the bridging nature of the three aryloxo ligands leaves vacant coordination sites on the metal centers. In contrast to Ba in the alkali/barium complexes, strontium in compounds **1–4** demonstrates a range of 4–10 for the total number of Sr– π contacts (upper limit 3.30 Å),³² suggesting that aside from the metal size, the orientation of the aryloxides and the phenyl substituents with respect to the metal centers influences the degree of these secondary interactions, which have binding modes of $\eta^4:\eta^2:\eta^1$ in **1**, $\eta^1:\eta^1:\eta^2:\eta^6$ in **2**, $\eta^3:\eta^1:\eta^2$ in **3**, and $\eta^1:\eta^1:\eta^2$ in **4**. Conversely, π coordination of calcium (upper limit 3.13 Å)³² in a $\eta^1:\eta^1:\eta^1$ fashion is consistently observed in **5–7**, with the shortest Ca–C contact being 2.865(3) Å. The alkali metals in **1–7** show the expected trend of their metal–arene interactions in descending down the group, with the largest alkali metal, cesium, having the most extensive coordination ($\eta^1:\eta^2:\eta^5:\eta^3$ in **4** and $\eta^5:\eta^1:\eta^2:\eta^3$ in **7**) with contacts ranging from 3.439(2) to 3.802(2) Å, which are within the typical range of Cs– π distances.³⁹ The M₂Ae(Odp)₄ structural type in **9** and **10** resulted in a reduced degree of π interactions for calcium and strontium compared with that in **1–7**. Similarly, this core structure also allows π stabilization of the lithium centers in **9** and **10** with a nearly equivalent degree of lithium– π interactions.

As a further illustration of the significance of metal– π -arene interactions, the coordination of thf to calcium (as in **8**) resulted in a marked reduction in the number of

(46) Hevia, E.; Henderson, K. W.; Kennedy, A. R.; Mulvey, R. E. *Organometallics* **2006**, *25*, 1778–1785.

(47) Fromm, K. M. *Chem. Commun.* **1999**, 1659–1660.

Table 7. TGA Data for **1**, **3–5**, **8–10**, a Family of M/Ba Compounds, and the Homometallic Compounds [Ca₂(Odpp)₄] and [Ba₂(Odpp)₄]

compound	stage of weight loss	temperature range (°C)	weight loss (wt %)	amount of residue (wt %)
[NaSr(Odpp) ₃]·PhMe, 1	I	108–127	10	15
	II	290–477	75	
[KSr(Odpp) ₃]·PhMe, 3	I	87–125	10	23
	II	256–494	67	
[CsSr(Odpp) ₃], 4	I	70–88	8	53
	II	262–430	18	
	III	485–562	21	
[Li ₂ Sr(Odpp) ₄]·PhMe, 9	I	107–126	6	28
	II	341–485	66	
[NaCa(Odpp) ₃]·PhMe, 5	I	61–125	8	6
	II	234–458	77	
[KCa(Odpp) ₃ (thf)]·PhMe, 8	I	97–132	8	15
	II	216–337	85	
[Li ₂ Ca(Odpp) ₄], 10	I	96–400	86	14
	II	350–603	12	
[Ca ₂ (Odpp) ₄]	I	96–539	89	11
[Ba ₂ (Odpp) ₄]	I	152–281	5	83
	II	350–603	12	
[NaBa(Odpp) ₃]·PhMe	I	97–120	6	29
	II	275–492	65	
[KBa(Odpp) ₃]·PhMe	I	99–120	8	39
	II	257–460	53	
[KBa(Odpp) ₃ (diglyme)]	I	116–140	15	16
	II	354–517	69	
[Li ₂ Ba(Odpp) ₄]·PhMe	I	333–490	61	39
[Li ₂ Ba(Odpp) ₄ (thf) ₂]·PhMe	I	100–150	17	27
	II	325–477	56	
[CsBa(Odpp) ₃]	I	75–100	6	33
	II	318–523	61	

calcium–arene interactions, from three in the donor-free species **6** to only one Ca–C contact [2.997(3) Å] in **8**. Consequently, the three bridging ligands in **8** incline more toward the potassium metal, conferring an increase in π bonding between the phenyl rings and the potassium metal (binding mode $\eta^3:\eta^6:\eta^6$) compared with the amount observed in the donor-free compound **6** (binding mode $\eta^6:\eta^4:\eta^3$). Gentle heating of **8** released thf, presumably resulting in the formation of **6**. As demonstrated in the thermogravimetric analysis (see below), loss of THF in **8** began at 97 °C and was complete at 132 °C. Similar donor loss was observed in [Li₂Ba(Odpp)₄(thf)₂] and [KBa(Odpp)₃(diglyme)], with thf being released from 100 to 150 °C and diglyme from 116 to 140 °C.¹⁹ The presumed formation of the respective donor-free species upon loss of the coordinated solvents supports the significance of metal– π interactions in the stabilization of the heterobimetallic compounds.

TGA Studies. Thermal stabilities and volatilities of representative heterobimetallic strontium and calcium complexes were investigated using thermogravimetric analysis under a 1 atm flow of nitrogen. The compounds were selected on the basis of their sharp melting points accompanied by uniform transitions from solid to liquid without apparent decomposition (see the Experimental Section). Another motivation for these investigations originated from the observation that crystalline samples of these compounds were deposited on the walls of the tube during their preparation, which can be an indication of mass transport. Relevant data on weight loss (wt %) upon heating and the corresponding stages of weight loss for the heterobimetallic compounds reported here and their barium analogues, as well as for the homometallic species [Ae₂(Odpp)₄] (Ae = Ba, Ca) for the sake of comparison, are summarized in Table 7. The weight

loss for some of the compounds occurred in two distinct stages. Stage I transpired over an extended temperature range (61–148 °C) and corresponds to the loss of the cocrystallite solvent toluene or, in the case of the solvated species, the loss of the donor. A common feature of the TGA results for the compounds was the significant weight loss (stage II) that generally occurred over the temperature range 200–500 °C. Compound **5** exhibited the least amount of residue (6%), suggesting its potential as a CVD precursor. Figure 7 displays the TGA plot of **5** in comparison with those for the related Na/Sr and Na/Ba compounds, which also exhibited the least amount of residue among the series of donor-free heterobimetallics. The small amount of residue may indicate vaporization of the molecular species, though sublimation studies and collection of other characterization data are underway in order to ascertain the compositions of the residue and the volatile substances. Notably, there was no direct relationship between thermal stability and the size of either metal, but it was evident that the calcium homologues generally showed the least amount of residue. A striking difference in the TGA profiles between the heterobimetallic species and the homometallic alkaline earth metal compounds was observed. Heating the dimeric complex [Ba₂(Odpp)₄] to 600 °C produced a weight loss of only 17% and gave black decomposition products, while [Ca₂(Odpp)₄] showed a steady weight loss upon heating, which started below 100 °C and left an 11% residue at 589 °C.

Comparison of the TGA profiles for the heterobimetallic solvated species with those for the donor-free derivatives revealed that the former showed a greater weight loss than the latter, indicating that loss of the donor does not produce oligomeric compounds, which often are associated with a lower volatility than compounds having low nuclearities. This

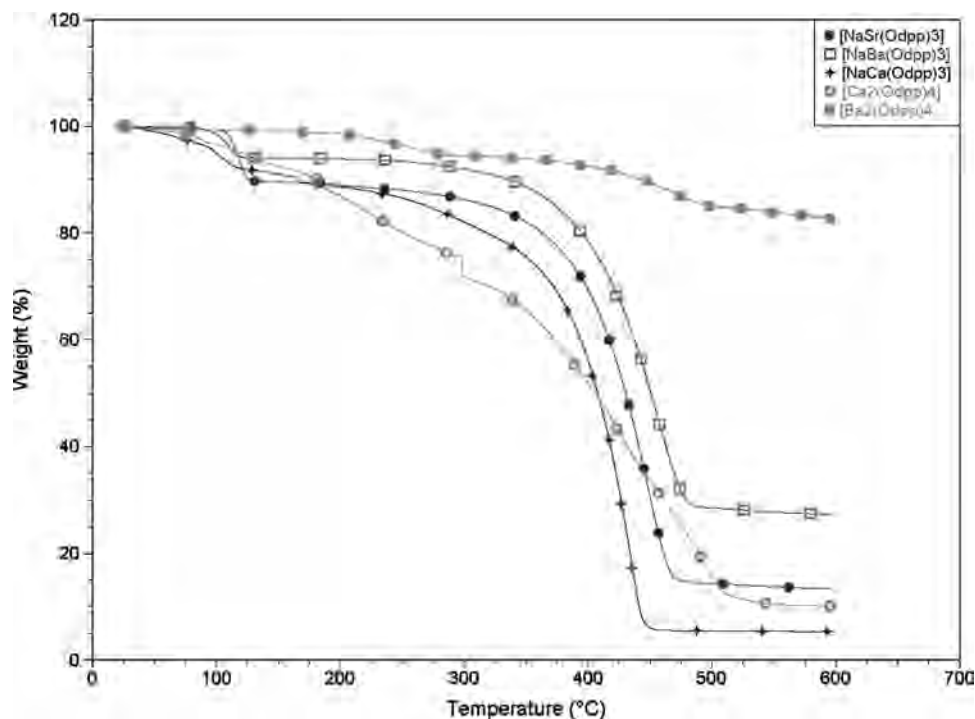


Figure 7. Comparison of TGA plots for the series of Na/Ae compounds and the homometallic compounds $[\text{Ca}_2(\text{Odpp})_4]$ and $[\text{Ba}_2(\text{Odpp})_4]$.

result further supports our assumption that the loss of the donor solvent in the complexes $[\text{Li}_2\text{Ba}(\text{Odpp})_4(\text{thf})_2]$ and $[\text{KBa}(\text{Odpp})_3(\text{diglyme})]$ leads to the formation of the corresponding donor-free species.¹⁹ Although there are no available data for the related donor-free K/Ca species for compound **8**, we presume that a donor-free species would be obtained. Further investigations, including sublimation studies and analytical procedures to identify the composition of the volatile materials and the residues, are necessary in order to ultimately establish the utility of these compounds as precursors for metal oxide thin films via the CVD process.

Conclusions

The findings in this work conclude our investigations of the rational synthesis and characterization of mixed alkali/alkaline earth metal systems using the Odpp^- ligand. We have demonstrated the unusual structural features of a series of heterobimetallic alkali/strontium and alkali/calcium complexes and compared them to those of a family of barium analogues. The donor-free compounds involving the alkali metals sodium, potassium, and cesium exhibit a unique cagelike structure consisting of three ligands doubly bridging

the metals, while compounds based on lithium show a core structure of two fused four-membered LiO_2Ae rings with consequent 2:1 alkali/alkaline earth metal stoichiometry. These structural trends also illuminate the subtle differences in the geometrical features of the compounds, as influenced by the size of the metal centers. Detailed analysis of the coordination modes and solvation of these compounds has further established the role of metal- π interactions in the stabilization of these compounds. Moreover, the successful preparation of these compounds has proven the far-reaching applications of the solid-state direct-metalation route in alkaline earth metal chemistry.

Acknowledgment. We gratefully acknowledge support from the National Science Foundation (CHE-0505863). Purchase of the X-ray diffraction equipment was made possible by grants from the National Science Foundation (CHE-9527858 and CHE-0234912), Syracuse University, and the W. M. Keck Foundation. Support from the Australian Research Council is also gratefully acknowledged.

IC702466D